

Micro Seismic Electret Generator for Energy Harvesting

T. Tsutsumino^{1*}, Y. Suzuki¹, N. Kasagi¹, K. Kashiwagi², and Y. Morizawa²

¹Department of Mechanical Engineering, The University of Tokyo
7-3-1 Hongo, Bunkyo-ku, Tokyo, 113-8656

²Asahi Glass Corporation
Hazawa-cho 1150, Kanagawa-ku, Yokohama, Kanagawa, 221-8757

Abstract

Evaluation of a micro electret generator for energy harvesting applications is presented. MEMS-friendly perfluoropolymer, CYTOP is adopted as high-performance electret material. In power generation experiments using a prototype seismic generator, maximum power output of 0.278 mW has been obtained with 1.2 mm_{p-p} in-plane oscillation at 20 Hz. Electrostatic force is calculated using one-dimensional electrostatic field model. It is found that the electrostatic force in the in-plane direction is almost constant irrespective to the direction of motion. When two separate generators with a 180° phase difference are integrated on a single chip, the horizontal force becomes smaller by two orders of magnitude, but exhibits different trends from velocity-damped or coulomb-damped resonant generators.

Keyword : Electret, Energy harvesting, Power Generation, Electrostatic Force

1. INTRODUCTION

Recently, energy harvesting device from environmental vibration attracts much attention in view of its possible applications to RFIDs and automotive sensors [1, 2]. Since the frequency range of vibration existing in the environment is below a few tens of Hz, electret power generators [3] should have higher performance than electromagnetic ones. However, since the power output obtained with previous electret generator prototypes is limited to a few tens of μW [4, 5], much larger power output should be demonstrated to make energy harvesting with electret generators feasible in real applications.

We recently discovered that MEMS-friendly amorphous perfluoropolymer, CYTOP can produce a very large surface charge density as a stable electret material [5, 6]. In the present study, we examine power generation performance of a prototype seismic generator with the CYTOP electret. In addition, we develop a generator model in order to investigate electrostatic force during its operation.

2. ELECTRET POWER GENERATOR

Figure 1 shows a schematic of the micro electret generator proposed in the present study. When vibration in the in-plane direction is applied, the seismic mass with electret undergoes a relative motion with respect to the counter electrode on the bottom substrate. Thus, the amount of the induced charge on the counter electrode is changed due to the change in the overlapping area, producing electric current in the external circuit. The seismic mass is supported by parylene high-aspect-ratio springs [7], which enable large amplitude oscillation and low resonance frequency.

Figure 2 shows a simplified model of the generator, where σ , d , and g are respectively surface charge density, thickness of the electret film, and gap between the electret and the counter electrode. The length x_1 represents the overlapping area be-

tween the electret film and the counter electrode. The parasitic capacitance C_p is assumed to be constant as described later. Using a simple capacitance model, Boland *et al.* [4] show that the maximum output power of electret power generator is proportional to the surface charge density squared σ^2 , and is increased with increasing the thickness of electret d . On the other hand, the optimal load resistance is independent of σ , but linearly dependent on d and g . Procedure for numerical analysis of the generator model is described in the following chapter.

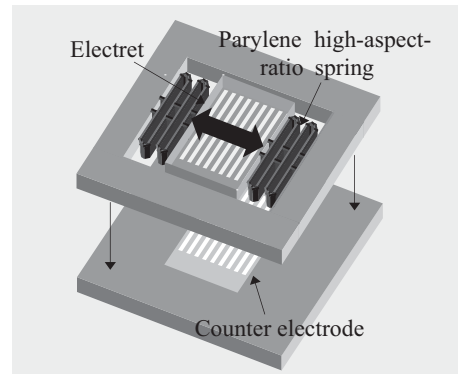


Fig. 1. Schematic of micro electret generator.

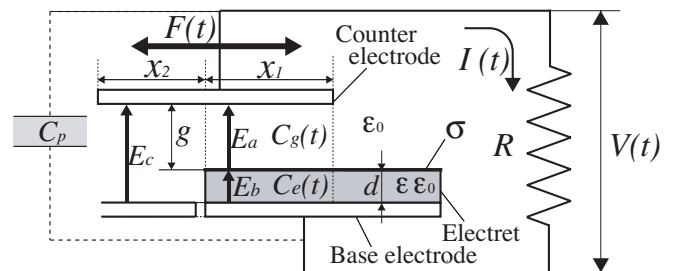


Fig. 2. Computational model of electret generator.

* Contact author : Tel. 81-3-5841-6419, Fax : 81-3-5800-6999, email : tsutsumino@thtlab.t.u-tokyo.ac.jp

Various kinds of materials have been proposed for electrets [8]. Among them, dielectric polymer materials, especially perfluoropolymer such as PTFE, are generally employed. Hsieh *et al.* [9] employ Teflon AF as the electret material for their MEMS microphone. In our previous study [5, 6], we have found that CYTOP (CTL-809M, Asahi Glass Co., Ltd.), which is also amorphous perfluoropolymer compatible with MEMS process, can exhibit surface charge density of 1.3 mC/m² for 15 μm-thick film. Since the surface charge density of CYTOP is 3 times larger than that of Teflon AF, 9 times larger output power can be expected when CYTOP is employed as the electret material.

3. NUMERICAL ANALYSIS OF ELECTRET GENERATOR

As shown in Fig. 2, one-dimensional electrostatic field is assumed. Applying Gauss's law at the electret surface, we get

$$-\varepsilon\varepsilon_0E_b + \varepsilon_0E_a = \sigma, \quad (1)$$

where E_a , E_b , ε , and σ are respectively electrostatic fields in the electret film and the air gap, relative permittivity of the electret material, and the surface charge density. With Kirchhoff's law, we get

$$V + dE_b + gE_a = 0, \quad (2)$$

and

$$V + (d + g)E_c = 0, \quad (3)$$

where V and E_c are respectively the output voltage and the electrostatic field between a counter electrode and a guard electrode.

The induction current $I(t)$ is given by the conservation of charge :

$$\sigma_{i1}bx_1 + \sigma_{i2}bx_2 + \int_0^t I(t) + C_p V = Q(const), \quad (4)$$

where σ_{i1} and σ_{i2} are the induced charges, which are respectively given by $\sigma_{i1} = -\varepsilon_0E_a$ and $\sigma_{i2} = -\varepsilon_0E_c$. The quantity b represents length of the electrodes.

Substituting Eqs. (1-3) into Eq. (4), a differential equation with respect to the output voltage $V(t)$ is obtained. Unlike more simplified form given by Tada [3], Eqs. (1-4) have no analytical solution. Thus, it is solved numerically under the same conditions with the present experiment shown below.

Considering the conservation of energy, the work done by the external force $F_x dx/dt$, power consumption at the load resistance V^2/R and the electrostatic energy E_s satisfy the following equation:

$$\frac{dE_s}{dt} - \left(\frac{V^2}{R} + C_p V \frac{dV}{dt} \right) + F_x \frac{dx}{dt} = 0, \quad (5)$$

where F_x is the force in the horizontal direction required for the oscillation. The electrostatic energy E_s can be computed with $V(t)$ and the overlapping area. Mitcheson *et al.* [10] investigated performance of three kinds of modelled generators, i. e., velocity-damped resonant, coulomb-damped resonant, and coulomb-force parametric generators. In the present study, we compute the force acting in our in-plane generator in order to examine the applicability of their models.

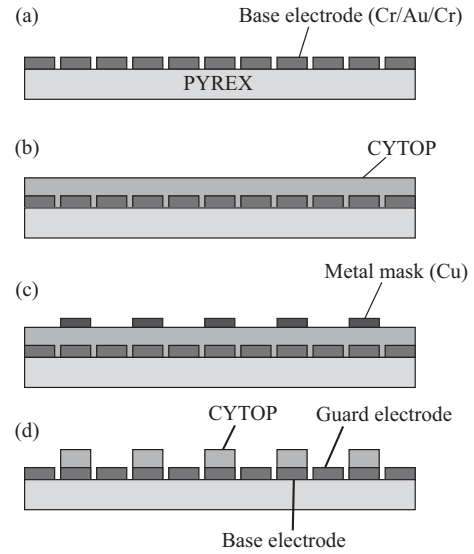


Fig. 3. Fabrication process of the electret plate : (a) Deposit and pattern base electrode (Cr/Au/Cr), (b) Spin-on and cure CYTOP, (c) Deposit and pattern metal mask (Cu), (d) O₂ plasma etch and remove metal mask.

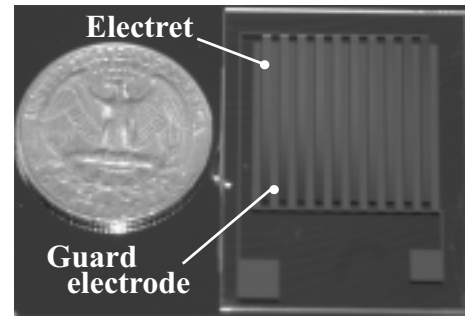


Fig. 4. Glass substrate with patterned electret.

Table 1. Condition of corona-charging.

Needle voltage	-8 kV
Grid voltage	-600 V
Temperature	120 °C
Charge time	10 min.

4. FABRICATION

For power generation experiments, we develop a prototype electret generator. Figure 3 shows the fabrication process of the electret plate. Firstly, Cr/Au/Cr (10/100/10 nm in thickness) thin films are deposited on a 0.7 mm-thick Pyrex wafer using an EB evaporator, followed by patterning with standard lithography and wet etching. Then, CYTOP (CTL-809M) is spun-on at a rotational speed of 1,000 rpm for 20 seconds and soft-baked at 100 °C for 30 minutes. This process is repeated 7 times to obtain a 20 μm-thick film, and is fully-cured at 185 °C for 1.5 hours. Next, copper is evaporated and patterned as the metal mask. Finally, the CYTOP film is etched by O₂ plasma with 100 W RF power for 60-70 minutes. The counter electrode is fabricated with a similar process. Figure 4 shows the patterned electret film with guard electrodes. The width of electret and guard electrodes is 150 μm, and the gap in be-

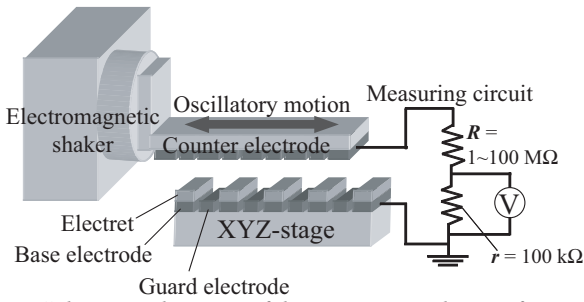


Fig. 5. Schematic diagram of the experimental setup for power generation.

Table 2. Capacitance between a patterned electret and a patterned counter electrode with a gap of 100 μm .

Overlapping area	Without guard electrodes		Theoretical value
	Without guard electrodes	With guard electrodes	
100%	39.8 pF	22.4 pF	17.7 pF
0%	25.4 pF	2.3 pF	0.0 pF

tween is 30 μm . The total area of the electret is 10 x 20 mm^2 .

The electret plate is then charged by corona discharge. The condition of corona-charging is shown in Table 1. The temperature during charging is kept at higher than the glass transition temperature of CYTOP. Average surface voltage of about -600 ~ -1000 V is obtained after this charging process.

5. POWER GENERATION EXPERIMENT

The setup for power generation experiment is shown schematically in Fig. 5, which consists of the electret plate, the counter electrode plate, an alignment stage, and an electromagnetic shaker (APS-113, APS Dynamics Inc.). The electret plate and the counter electrode plate are respectively fixed to the shaker and the alignment stage. The gap is measured with a laser displacement meter (LC-2430, Keyence Inc.). The counter electrode plate is moved sinusoidally in the in-plane direction by the shaker. In order to measure the output voltage for various external loads, a simple measuring circuit with a voltmeter and two resistors in series is employed.

For obtaining large capacitance and thus large output power, it is necessary to reduce the gap between the electret and counter electrode plates. However, electric breakdown of the air gap between the plates should occur, since the surface potential of the electret is higher than -600 V, which is close to the breakdown voltage of air for a 50 μm gap. In the present study, SF6 gas, which has 2.5 times larger breakdown voltage than air, is introduced into the gap.

Table 2 shows the capacitance between the electret and the counter electrode plates for the gap $g = 100 \mu\text{m}$. Without the guard electrode, the capacitance measured for both 100% and 0% overlap are significantly larger than their theoretical values of 17.7 pF and 0 pF. On the other hand, with the guard electrode, the parasitic capacitance is significantly decreased, and the capacitance for 0% overlap drops to 2.3 pF.

The distance between the top and bottom glass substrate and the oscillation amplitude are respectively set to 40 μm and

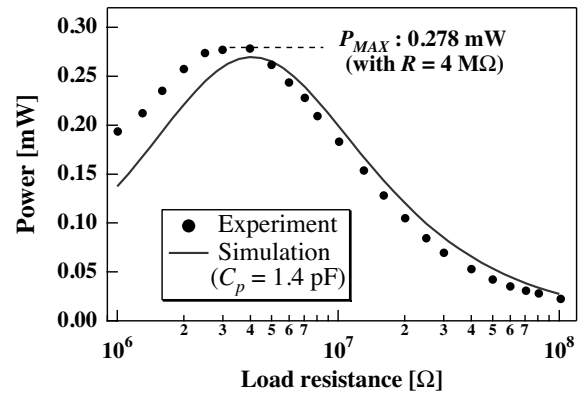


Fig. 6. Power output versus external load at $f = 20\text{Hz}$.

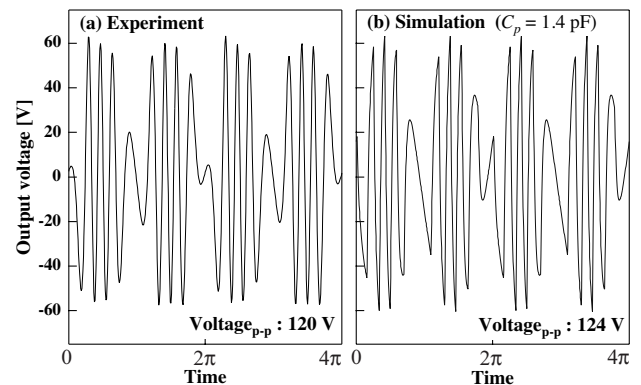


Fig. 7. Time trace of the output voltage at $f = 20\text{Hz}$ and $R = 4\text{M}\Omega$. (a) Experiment, (b) Simulation result with the generator model.

1.2 $\text{mm}_{\text{p-p}}$. Since the thickness of electret is 20 μm , the gap between the electret and the counter electrode surface is 20 μm . The theoretical capacitance for the 100 % overlap is 88.5 pF. The oscillation frequency f is set to 20 Hz. The surface potential of the electret is about -600 V.

Figure 6 shows the output power versus the external load R . Maximum output power of 0.278 mW is obtained at $R = 4\text{M}\Omega$. Therefore, power generation on the order of 1 mW from low-frequency vibration should be feasible for electret generators. In the present numerical simulation, the parasitic capacitance is estimated with a least-square fit to the experimental data, and is set to $C_p = 1.4\text{pF}$. Numerical results under the same condition with the experiment are in reasonable agreement with the experimental data.

Figure 7 shows the time trace of the output voltage obtained with $R = 4\text{M}\Omega$. Since the amplitude is 8 times larger than electrode width, high-frequency oscillation at 160 Hz is observed. The peak-to-peak voltage is as large as 120 V. Again, the simulation results are in good agreement with the experimental data.

It is now clear that the present model can mimic the response of the electret generator with sufficient accuracy. Figure 8 shows the computational results for the electrostatic force acts in the in-plane (horizontal) direction together with the oscillation velocity during one cycle of the sinusoidal movement. It is found that large force of 10 N appears alternately in oppo-

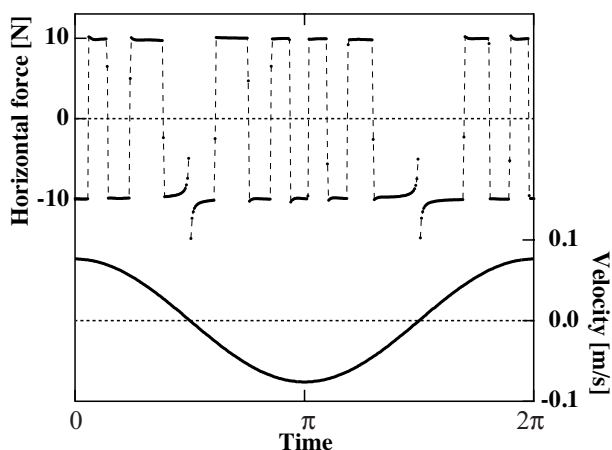


Fig. 8. Time trace of horizontal force and the plate velocity.

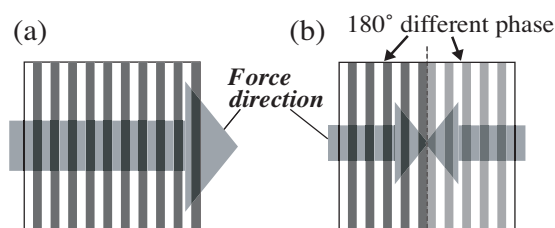


Fig. 9. (a) Arrangement of electret poles for the present experiment, (b) Arrangement of electret poles with two separate circuits 180° out-of-phase.

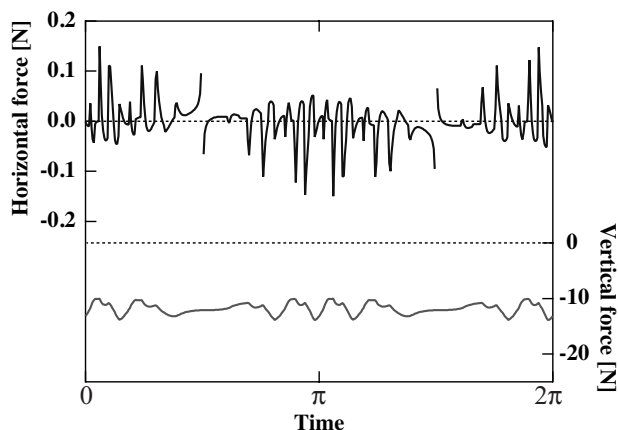


Fig. 10. Time trace of the electrostatic force in the horizontal and vertical direction.

site directions. The force direction is switched every time the poles of the counter electrode pass through the electret poles.

In order to reduce this large horizontal electrostatic force, an arrangement of electret poles shown in Fig. 9 is proposed, where two separate generators with a 180° phase difference are integrated on a single chip. Figure 10 shows the horizontal and vertical forces, when the configuration shown in Fig. 9 is adopted. Large horizontal force shown in Fig. 8 is almost cancelled out, and relatively-small force on the order of 0.1 N is left. Note that this counteractive force of the in-plane electret generator is not proportional to the velocity, and exhibits much different trends from those of the previous models [10]. On the other hand, in the vertical direction, large and almost constant attraction force of 12 N acts independently of electrode move-

ment. This is because the surface potential of the electret film (~600V) is much higher than the time-varying voltage of the counter electrode.

6. CONCLUSION

We develop a MEMS-friendly electret film using CYTOP, and examine its performance with a prototype micro seismic generator. We also evaluate the electrostatic force with a simplified model. The following conclusions can be derived:

- (1) The maximum output power of 0.278 mW and peak-to-peak voltage of 120 V have been obtained at 20 Hz oscillation with 4 MΩ external load. Therefore, energy harvesting on the order of 1 mW is feasible with electret generators.
- (2) The present generator model can mimic the response of the in-plane electret generator with sufficient accuracy.
- (3) When two separate generators with a 180° phase difference are integrated on a single chip, the in-plane electrostatic force becomes smaller by two orders of magnitude. The trend of the in-plane force is much different from previous models, such as velocity-damped resonant generator.

This work is supported through the New Energy and Industrial Technology Development Organization (NEDO) of Japan. Photomasks are made using the EB writer F5112+VD01 at the University of Tokyo VLSI Design and Education Center (VDEC), which is donated by ADVANTEST Corporation.

REFERENCE

- [1] J. A. Paradiso, and T. Starner, "Energy Scavenging for Mobile and Wireless Electronics," IEEE Pervasive Computing, Vol. 4, pp. 18-27, 2005
- [2] S. Roundy, P. K. Wright, and J. Rabaey, "A Study of Low Level Vibration as a Power Source for Wireless Sensor Nodes," Computer Communication, Vol. 26, pp. 1131-1144, 2003.
- [3] Y. Tada, "Theoretical Characteristics of Generalized Electret Generator, using Polymer Film Electrets," IEEE Trans. Electrical Insulation, Vol. 21, pp. 457-464, 1986.
- [4] J. Boland, C.-H. Chao, Y. Suzuki, and Y.-C. Tai, "Micro Electret Power Generator," Proc. 16th IEEE Int. Conf. MEMS, Kyoto, pp. 538-541, 2003.
- [5] Y. Arakawa, Y. Suzuki, and N. Kasagi, "Micro Seismic Power Generator using Electret Polymer Film," Proc. PowerMEMS 2004, Kyoto, pp. 187-190, 2004.
- [6] T. Tsutsumino, Y. Suzuki, N. Kasagi, and Y. Sakane, "Seismic Power Generator using High- Performance Polymer Electret," IEEE Int. Conf. MEMS 2006, Istanbul, pp. 98-101, 2006.
- [7] Y. Suzuki, and Y.-C. Tai, "Micromachined High-Aspect-Ratio Parylene Spring and Its Application to Low-frequency Accelerometer," IEEE J. MEMS, Vol. 15, pp. 1364-1370, 2006.
- [8] G. M. Sessler, Electrets 3rd Edition, Laplacian Press, 1998.
- [9] W. H. Hsieh, T. J. Yao, and Y.-C. Tai, "A High Performance MEMS Thin-film Teflon Electret Microphone," Int. Conf. Solid-state Sensors Actuators, Sendai, pp. 1064-1067, 1999.
- [10] P. D. Mitcheson, T. C. Green, E. M. Yeatman, and A. S. Holmes, "Architectures for Vibration-Driven Micropower Generators," IEEE J. MEMS, Vol. 13, pp. 429-440, 2003.